Simulation of Biocube-Fluid Mixture Using Combined Formulation

Hyoung-gwon Choi*
Corresponding Author, Full-time Lecturer, Department of Mechanical Engineering, Seoul National University of Technology, Seoul 139-743, Korea
Myeong-ho Lee, Ho Taek Yong
Department of Mechanical Engineering, Seoul National University of Technology, Seoul 139-743, Korea

Combined formulation developed for the fluid-particle mixture is introduced to simulate the biocube-fluid mixture flow, which is utilized for sewage disposal. Some tricky boundary conditions are introduced in order to simulate the effect of screen wall and air bubble, which is injected from the bottom of sewage reservoir. It has been shown that a circulated flow pattern, which was observed in experiment, is reproduced from the present numerical simulation. Furthermore, the effect of biocube density on the distribution pattern of biocube is also studied. It has been shown that a biocube whose density is slightly smaller than that of surrounding fluid or neutrally buoyant one are optimal for the uniform distribution of biocube.

Key Words : Combined Formulation, Biocube-Fluid Mixture, Boundary Conditions

Nomenclature

a_{ij} : Coefficient associated with u-velocity of fluid in combined formulation
b_{ij} : Coefficient associated with v-velocity of fluid in combined formulation
c_{ij} : Coefficient associated with pressure in combined formulation
C_d : Drag coefficient
e_x, e_y, e_z : Unit vector in x, y, z direction
F_{drag} : Drag
g : Gravity
G : External force
H^1 : A function space which has the square integrable first derivative
I : Identity matrix
I : Moment of inertia
L^2 : A space which has the square integrable function
m : Mass of a biocube
M : Matrix associated with the motion of a biocube
p : Pressure
R : Radius of air-bubble
Tr : Traction acting on a biocube
u : x-component of fluid velocity
U : Biocube velocity
$\vec{U}_p$: Translation velocity of biocube
$\vec{u}$: Fluid velocity
$\vec{u}_m$: Mesh velocity
v : y-component of fluid velocity
$\vec{x}$: Position vector of a point on a biocube surface
$\vec{X}_c$: Position vector of the mass center of a biocube Greek Symbols

Greek Symbols

μ : Viscosity
ρ : Density
τ : Viscous stress
Γ : Boundary
Ω : Angular velocity of bicube

* Corresponding Author,
E-mail : hgchoi@snut.ac.kr
TEL : +82-2-970-6312; **FAX** : +82-2-949-1458
Corresponding Author, Full-time Lecturer, Department of Mechanical Engineering, Seoul National University of Technology, Seoul 139-743, Korea. (Manuscript **Received** May 30, 2003; **Revised** May 6, 2004)

Superscripts

T : Transpose
n : Time step

Subscripts

p : Particle (Biocube)
g : Dirichlet boundary condition
w : Surrounding fluid

1. Introduction

Environmental technology has been emerging as one of the most highlighted technologies as the demand of healthy life increases rapidly with the advent of 21 century. Accordingly, various new technologies have been introduced to solve the problems related to the soil, air and water pollution. In the case of water pollution, several techniques have been used to effectively remove both nitrogen and phosphorus which are present in a sewage reservoir. Biocube-fluid mixture with air-bubble-jet system (Kolon, 2000) has been introduced to remove the noxious chemicals in a reservoir rapidly and uniformly. A biocube of cubical shape, which is made of porous material, is used in order to trap microbes that destroy the noxious chemicals.

In the present study, we have adopted a modified version of the finite element code (Choi, 2000) developed by the first author in order to simulate the interaction of biocubes in the sewage reservoir with the air bubbles ejected from the bottom of the reservoir. The simulation of the present study is performed to qualitatively predict the behaviour of the biocubes in the system. The interaction of biocubes with the air bubbles results in the uniform distribution of them in sewage reservoir, leading to the uniform and rapid reduction of the noxious chemicals in the sewage reservoir. The effect of air-bubble-jet, which is ejected asymmetrically from the bottom of the sewage reservoir, on the distribution of biocubes is studied in a qualitative way. Furthermore, the effect of the biocube density and the wall height of the screen on the right side of a reservoir on the distribution of biocubes are also presented through the two-dimensional combined simulation of the fluid-particle mixture. The numerical method used in the present study is based on the combined formulation proposed by Hesla (1990) and later implemented by Glowinski et al. (1999), where the motion of the each particle is simultaneously solved together with the motion of the fluid that is governed by the Navier-Stokes equations. Hu (1996) firstly adopted the combined formulation for the unsteady numerical simulation of fluid-solid particle system using unstructured mesh. Choi and Joseph (2001) also adopted the combined formulation for the unsteady numerical simulation of fluidization by lift of 300 particles driven by pressure gradient in a two-dimensional channel flow. It needs to be noted that most of previous researches on two phase flows have been based on data obtained by experiment or modeling (Kim, 2002, Lim and Han, 2003) since the direct numerical simulation of a two-phase flow such as the present combined approach is very complicated as well as expensive. As for the experimental study of fluid-particle mixture, Ahn et al. (2002) studied the characteristics of fluid flow and heat transfer in a fluidized bed heat exchanger with circulating particles.

In section 2, the detailed description of the numerical method used in this study is given emphasizing some simplified tricky boundary conditions without which the simulation of this complicated simulation is impossible. In section 3, some numerical results are given with respect to the effect of biocube density, the wall height of the screen and boundary conditions employed on the biocube distribution, respectively.

2. Numerical Method

2.1 Problem description and boundary conditions

The schematic of the problem to be simulated in the present study is shown in Fig. 1. The polluted fluid in reservoir is transported to the next reservoir through holes of screen which have a smaller diameter than biocube. As shown in Fig. 1, air bubbles are ejected from the pipeline located at the bottom of the reservoir in order to

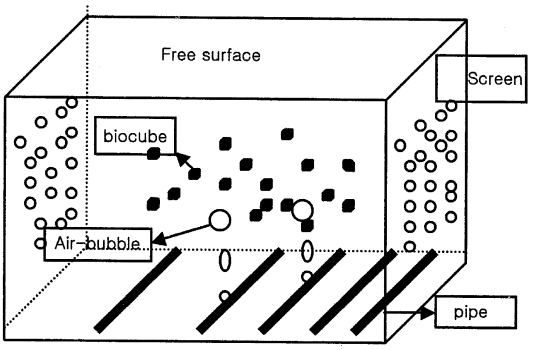

Fig. 1 Schematic of biocube plus air-bubble system in a channel flow with permeable screen

generate swirls in the reservoir. The asymmetric distribution of the pipeline, where air bubbles are produced, generates a swirl counter-clockwise. The role of the counterclockwise swirl is to distribute biocubes uniformly in the reservoir preventing the concentration of them near the right screen.

In the present study, a simplified two-dimensional approach of the biocube interaction with internal flow with screen and air bubbles is performed to qualitatively investigate both the motion and the distribution of the biocubes. The cubical type biocube is simplified by two-dimensional circle as shown in Fig. 2 because the unstructured mesh near biocube is so much distorted when two-dimensional square is used that the unsteady computation with moving grid is not possible especially when the number of biocube is great. In the present combined numerical simulation of the biocube-fluid mixture, an unstructured mesh is generated around each biocube and then the motion of fluid is solved together with that of each biocube simultaneously. This implicit type approach is based on the combined formulation proposed by Hesla. The method can be said to be "implicit" in the sense that the motion of biocube particle is solved with the motion of fluid at the same time instead of solving the motion of biocube separately with the calculated traction around each biocube which is obtained in a post processing step after the calculation of the flow field. Therefore, the unknown vector of the globally assembled matrix includes both the pressure and velocity field of the flow field and the translation and angular velocity of each biocube. Fig. 3 shows the simplified boundary conditions used in the present study. The inlet flow through the screen of the reservoir is assumed to be uniform. The outlet screen with holes is modeled by the intrinsic feature of P2P1 finite element, where velocity variables are interpolated by quadratic shape function and pressure variable by linear shape function, because lots of grid points are necessary when each hole is represented by an unstructured mesh. Utilizing the feature of P2P1 finite element, the screen with holes is roughly modeled by imposing no-slip and traction-free boundary condition, respectively on a vertex node and mid-node of each finite element on the screen wall. At the free surface, the following boundary condition is employed.

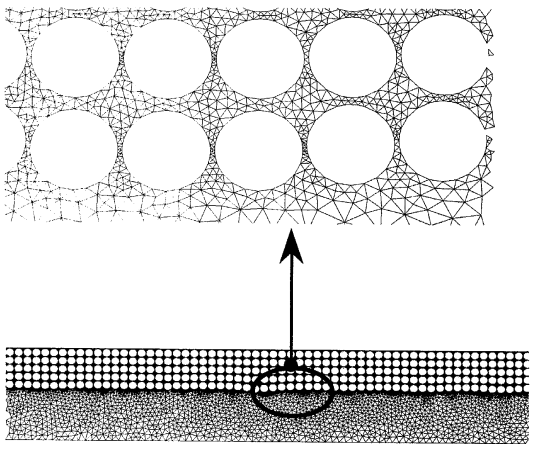

Fig. 2 Unstructured mesh around particles

Boundary condition at free surface :

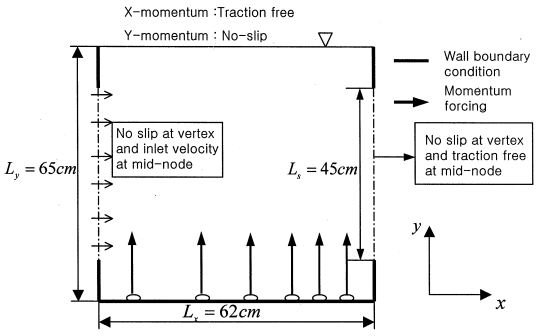

Fig. 3 Boundary conditions for two-dimensional calculation of biocube-fluid mixture

Traction free for the x-momentum equation and $v=0$ for the y-momentum equation.

This boundary condition is based on the assumption that both the surface tension and the normal velocity at free surface are negligible. This boundary condition is a kind of approximation to avoid the complexity of fluid motion at free surface and reproduce the experimental result well qualitatively.

Two following boundary conditions are considered for the bottom surface, from which air-bubbles are ejected.

Two boundary conditions tested at bottom surface:

(Case-I) A rising velocity of air-bubble ejected from the bottom is replaced by the fluid velocity at the boundary.

(Case-II) Air-bubble ejected from the bottom is replaced by an appropriate momentum forcing.

The motion of air-bubble interacting with biocube may be directly solved by using a numerical technique of multiphase flow. For instance, level set (Sussman et al., 1994) can be employed. However, the direct numerical simulation of the air-bubble interaction with biocube particle is not considered in this study due to the formidable amount of computation.

2.2 Governing equation and finite element formulation of biocube-fluid mixture

The governing equations are the incompressible Navier-Stokes equations coupled with the motion of each biocube.

$$\nabla\cdot\vec{u}=0 \tag{1}$$

$$\rho\frac{D\vec{u}}{Dt}=\nabla\cdot\sigma,\ \sigma=-p\mathbf{I}+\tau \tag{2}$$

$$\begin{aligned} M\frac{dU^{n+1}}{dt}&=G(\textit{body force})+Tr\\ &=G(\textit{body force})+\sum a_{ij}u_j+\sum b_{ij}v_j+\sum c_{ij}p_j \end{aligned} \tag{3}$$

where, $M=\begin{bmatrix} m & 0 & 0\\ 0 & m & 0\\ 0 & 0 & I \end{bmatrix}$ $U=\begin{bmatrix} u_p\\ v_p\\ \Omega_p \end{bmatrix}$ and

$\vec{u}=\vec{U}_p+\Omega_p\times(\vec{x}-\vec{X}_c)$ on Γ_p

where, in Eqs. (1) and (2), $\vec{u}$ is the fluid velocity and $\mathbf{I}$ is the identity matrix and τ is the viscous stress given by $\mu(\nabla+\nabla\vec{u}^T)$. In Eq. (3), Tr is the traction acting on the biocube surface by fluid, which is the sum of pressure and viscous stress. I, m, $\vec{U}_p$, Ω_p, Γ_p denote moment of inertia, mass, translation and angular velocity, and the boundary of each biocube, respectively. $\vec{x}$, $\vec{X}_c$ represent the position vectors of the node at biocube surface and the center of biocube, respectively, and $\vec{U}_p=(u_p,\ v_p)$.

In the present unsteady combined computation of fluid-particle mixture, the traction (Tr) in Eq. (3), which is a function of both velocity and pressure field, is evaluated at the current time step 'n+1' rather than the previous time step 'n'. This is the key point of the present combined formulation and thus it can be said to be an implicit method with respect to the treatment of the motion of particle. Utilizing the combined formulation proposed by Hesla (1990), the following Galerkin weak formulation is derived from Eqs. (1) ~ (3).

Find $\vec{u}_h\in H_h^1$, $p\in L_h^2$, $\vec{U}_p\in R\times R$, $\Omega_p\in R$ *such that*

$$\begin{aligned} &\int_\Omega\left[\vec{w}\cdot\rho\frac{D\vec{u}}{Dt}+\nabla\vec{w}:\sigma\right]d\Omega-\int_{\Gamma-\Gamma_p}\vec{w}\cdot\sigma\cdot\vec{n}d\Gamma\\ &+\sum_p\delta U_p\left(M\frac{dU}{dt}-G_p\right)\\ &+\int_\Omega q_h\nabla\cdot\vec{u}_h d\Omega=0 \ \textit{for all admissible functions} \end{aligned} \tag{4}$$

$w_h\in V_h$, $q_h\in L_h^2$

$V_h=\{\,w_h|\ w_h\in H_h^1$ *on* $\Omega-(\Gamma_g\cup\Gamma_p)$,

$w_h=0$ *on* Γ_g, $w_h=\delta U_p+\delta\Omega_p\times(\vec{x}-\vec{X}_c)$ *on* $\Gamma_p\,\}$

P2P1 triangular finite element is used to meet the well known Ladyshenskaja-Babushka-Brezzi (LBB) constraint. In a standard discretization, test and trial spaces for velocity and pressure cannot be chosen arbitrarily, but they have to meet the Ladyshenskaja-Babushka-Brezzi (LBB) condition. Standard methods become unstable if the LBB condition is violated. The numerical procedure used in the present study can be summarized as follows:

① The fluid variables (pressure and velocity) are obtained together with the translation and angular velocity of each biocube simultaneously by solving the following global matrix.

$$\begin{bmatrix} A_{uu} & A_{uv} & B_u & C_{uU_p} & 0 & C_{u\omega_p} \\ A_{vu} & A_{vv} & B_v & 0 & C_{vV_p} & C_{v\omega_p} \\ (B_u)^T & (B_v)^T & 0 & 0 & 0 & 0 \\ D_{U_pu} & D_{U_pv} & E_{U_pp} & m_p & 0 & 0 \\ D_{V_pu} & D_{V_pv} & E_{V_pp} & 0 & m_p & 0 \\ D_{\omega_pu} & D_{\omega_pu} & E_{\omega_pp} & 0 & 0 & I_p \end{bmatrix} \begin{bmatrix} u \\ v \\ p \\ u_p \\ v_p \\ \Omega_p \end{bmatrix} = \begin{bmatrix} f_u \\ f_v \\ 0 \\ g_{U_p} \\ g_{V_p} \\ g_{\omega_p} \end{bmatrix} \quad (5)$$

In Eq. (5), submatrices denoted by C represent the kinematic constraint satisfied at the biocube surface written as follows:

$$\vec{u} = u_p e_x + v_p e_y + \Omega_p e_z \times (\vec{x} - \vec{X}_c) \quad (6)$$

On the other hand, submatrices denoted by D and E represent the tractions acting on a biocube surface by pressure and viscous stress. It should be noted here that ALE (Arbitrary Lagrangian Eulerian) algorithm is adopted in the weak formulation (4) since each biocube is freely moving interacting with the surrounding fluid flow. Therefore, the momentum equations are to be modified accordingly. For instance, the x-momentum equation is to be modified as follows:

$$\rho\left(\frac{\partial u}{\partial t} + (\tilde{u}\cdot\nabla)\, u\right) = -\frac{\partial p}{\partial x} + \mu\nabla^2 u + G_x \quad (7)$$

where $\tilde{u} = \vec{u} - \vec{u}_m$

$$L\vec{u}_m = 0$$

$$\textit{Boundary condition}: \ \vec{u}_m = \vec{u}_{\Gamma_p} \ \textit{on} \ \Gamma_p, \quad \vec{u}_m = \vec{u}_{\Gamma_g} \ \textit{on} \ \Gamma_g \quad (8)$$

The mesh velocity in Eq. (7) is obtained by solving the Laplacian equation with the appropriate boundary condition given in Eq. (8) in order to obtain a smoothly varying element size. In Eq. (8), L is the Lapacian operator.

② A globally assembled matrix of Eq. (5) is to be solved in order to obtain both the flow field and the velocity of each biocube. At this stage, AILU (Adapted Incomplete LU factorization) preconditioner proposed by Nam et al. (2002) is adopted to accelerate the convergence of BiCGStab (Bi-Conjugate Gradient Stabilized) solver, which was proposed by van der Vorst in 1996.

③ The position of each biocube is updated from the new translation velocity obtained from step (2).

④ Remeshing/interpolation is conducted if the unstructured mesh at step (3) is too distorted. Otherwise, go to the step (1) in order to obtain the new velocity field at the next time step.

3. Numerical Results and Discussion

3.1 The effect of boundary condition (Air-bubble ejected from the bottom)

Two boundary conditions are tested to simulate the air-bubble jet ejected from the bottom. In the Case-I, the air-bubble jet is replaced by a jet velocity imposed where the air-bubble jet is ejected. The jet velocity has been calculated based on the following assumptions:

① The diameter of an air-bubble is constant

② The drag experienced by an air-bubble is balanced by the buoyancy force.

Then, from the definition of the drag:

$$F_{drag} \cong C_d \frac{1}{2} \rho_w A v^2 \quad (9)$$

Using the assumption that the drag is balanced by the buoyancy force:

$$C_d \frac{1}{2} \rho_w \pi R^2 v^2 \sim \frac{4}{3} \pi R^3 \rho_w g \quad (10)$$

where, ρ_w is the density of the surrounding fluid and R is the radius of the bubble. From the Eq. (10), we obtain the following formula when the diameter of the bubble is 1 mm.

$$v_b \sim 16 \frac{1}{\sqrt{C_d}} \quad (11)$$

Since the drag coefficient is the function of the velocity, the rising velocity (jet velocity) is derived by trial and error. The calculated rising velocity of air-bubble is about 17cm/sec. The mainstream velocity of sewage through the hole of screen is about 1cm/sec. In the Case-I, due to the rising velocity imposed at the bottom, a normal velocity component at free surface has a non-zero value by continuity constraint, which is not consistent with the physics claimed in section 2. Although it is not shown in the present paper, a preliminary calculation with this boundary condition has shown that some small vortices appear near the bottom of the reservoir. However, the primary counterclockwise vortex shown in Fig. 4 never appears, which is observed in experiment

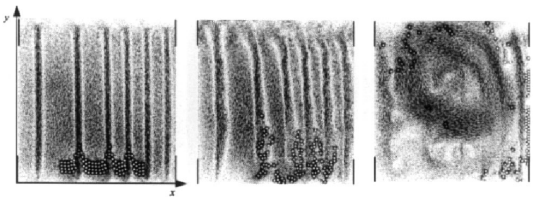

(a) $t\sim$1sec (b) $t\sim$3sec (c) $t\sim$15sec

Fig. 4 Flow field and neutrally buoyant biocube distribution with time

(Kolon, 2000). Therefore, in the present numerical experiment, we have used Case-II in order to simulate the air-bubble jet. The magnitude of momentum forcing imposed inside the reservoir has been obtained by trial and error such that the magnitude of upward velocity of surrounding fluid caused by the momentum forcing is close to the rising velocity of air-bubble derived from Eq. (11) when biocubes are absent.

It is really true that we should use the direct simulation of the motion of rising bubbles combined with fluid-particle mixture in order to exactly simulate the present problem in a general way. We might use an appropriate numerical technique such as level-set for the simulation of bubble-in-liquid. However, we have not had that kind of code yet and as far as we know, there is no reported work of that kind in the literature. Therefore, we have no other choice to use the "momentum forcing approach", which is used in some commercial code to simplify some problems of high complexity.

At free surface, zero velocity is used for y-momentum equation and zero traction for x-momentum equation. In the present computation, hundred biocubes are simulated by direct numerical simulation of the fluid-biocube mixture. The densities of surrounding fluid and biocube are the same as $1.0g/cm^3$ in the simulation shown in Figs. 4$\sim$5. The diameter of biocube is $1.0cm$ and the size of the reservoir is $62cm\times65cm$. The dynamic viscosity of fluid is given as $0.1g/cm\cdot sec$. Fig. 4-(a) and Fig. 4-(b) show the flow field and the distribution of biocubes at the early stage of computation. It is shown that upward velocity is generated inside a reservoir due to the momentum forcing and that biocubes move upward

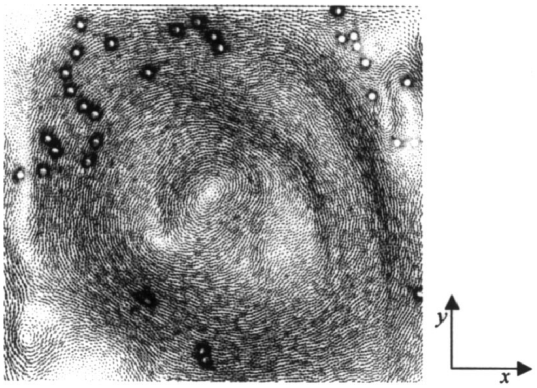

Fig. 5 Velocity field near the center of the primary vortex at t$\sim$40 sec

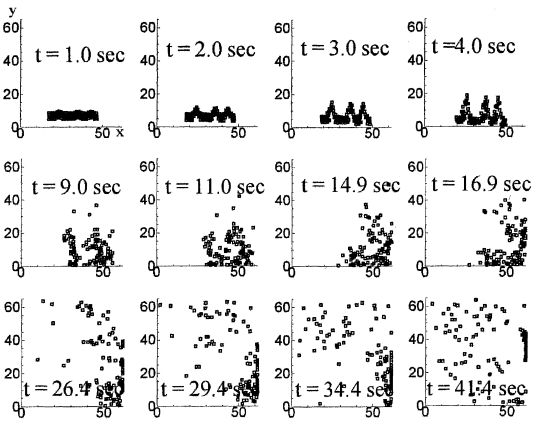

Fig. 6 Biocube distribution with time for the neutrally buoyant case

along each jet generated by the momentum forcing. Fig. 4-(c) shows the flow field and the distribution of biocubes when the flow field is nearly developed. It is clearly shown that the large counterclockwise vortex occupies most of the reservoir. Therefore, it can be said that most of biocubes are captured inside the primary vortex as the volume fraction of biocubes increases. It is shown in Fig. 4-(c) that some of biocubes hang over near the screen hole due to the mainstream fluid velocity through screen holes. Fig. 5 clearly shows a counterclockwise velocity field near the center of the primary vortex. Fig. 6 shows the distribution of biocubes with time. It is shown that more biocubes tend to distribute uniformly as the primary swirl becomes stronger as time goes on.

3.2 Wall effect at the upper and lower part of the screen

As shown in Fig. 6, some of biocubes still hang over near screen holes due to the inertia of the mainstream flow near holes. In order to wash out some of biocubes hung over screen holes, walls are installed at the upper and lower part of the screen as shown in Fig. 7. As shown in Fig. 7, local vortices generated near those walls tend to wash out biocubes hung over near the screen walls. This happens because the upward velocity of the surrounding fluid is larger than that of the mainstream velocity inside the reservoir.

3.3 Effect of biocube-density on the distribution pattern

It has been shown from the present simulation that some of biocubes reside inside the primary vortex when the biocube is neutrally buoyant. Note that biocube density used in the simulation of Figs. 4~5 is the same as that of surrounding fluid. However, it is shown that a portion of biocubes aggregate near the screen hole due to the mainstream flow through holes. In order to see the effect of biocube density on the biocube distribution pattern, the same kind of numerical simulation has been performed with two different biocube densities : 0.99g/cm^3 and 1.02g/cm^3. Fig. 8 shows the velocity fields as well as biocube distributions with time when the biocube density is 1.02g/cm^3. Fig. 9 shows biocube distribution with time for the biocube density of 1.02g/cm^3. The interaction of gravity force of biocube acting downward with the momentum forcing and the mainstream flow (from the left screen to the right screen in Fig. 8) seems to be very complex. Unexpectedly, most of biocubes move against the mainstream flow piling up near the lower left corner of the reservoir. Although some of biocubes detach from a pile of biocubes in the corner

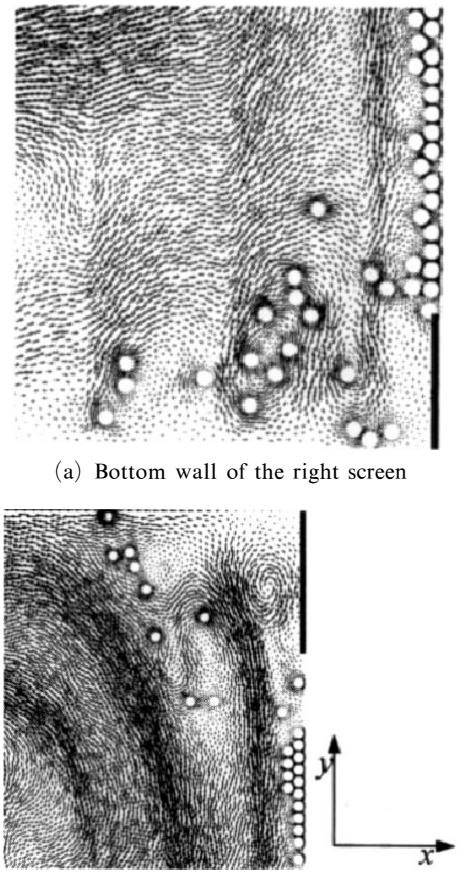

(a) Bottom wall of the right screen

(b) Top wall of the right screen

Fig. 7 Wash-out near the (a) bottom and (b) top screen walls

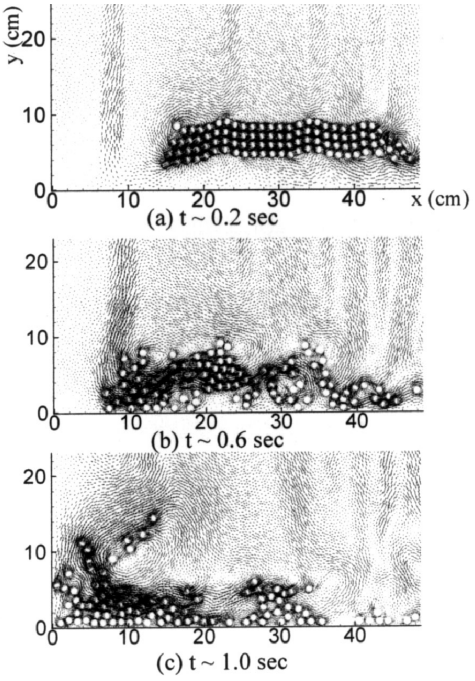

Fig. 8 Flow field and biocube distribution with time for biocube density=1.02g/cm^3

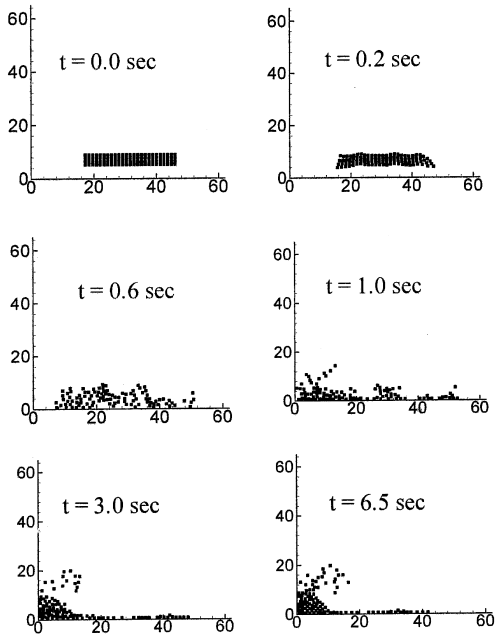

Fig. 9 Biocube distribution with time for biocube density=1.02g/cm^3

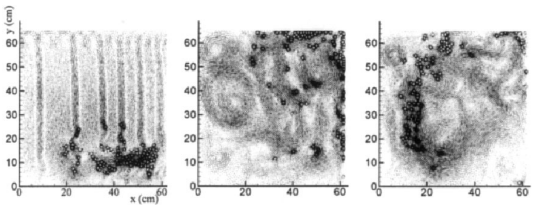

(a) t=4.0 sec (b) t=15.0 sec (c) t=4.0 sec

Fig. 10 Flow field and biocube distribution with time for biocube density=0.99g/cm^3

by momentum forcing (air-bubble), they don't move toward the center of the primary vortex because they are captured by a small vortex as shown in Fig. 8-(c). Fig. 10 shows a series of velocity fields and biocube distributions with time when the biocube density is 0.99g/cm^3. Fig. 10-(a) shows the velocity field and the corresponding biocube distribution at the early stage of computation. Compared with Fig. 4-(a) of the neutrally buoyant case, biocubes rise more rapidly along the air-bubble-jet due to buoyant force acting upward. Fig. 10-(a) also reveals that a series of vortex are generated along the jet in a very complicated way. In Fig. 10-(b), most of biocubes seem to float on the reservoir due to

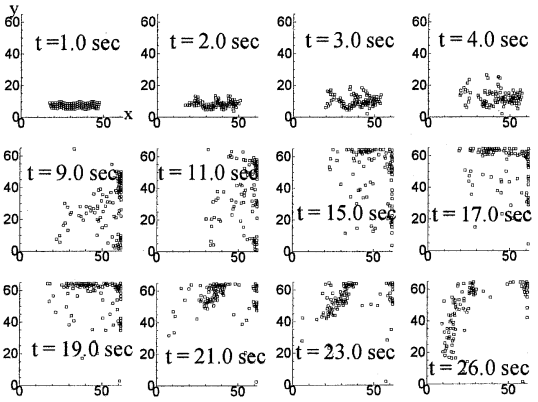

Fig. 11 Biocube distribution with time for biocube density=0.99g/cm^3

buoyant force although a counterclockwise primary vortex appears near the center of reservoir. However, Fig. 10-(c) shows that eventually, most of biocubes are captured by the interaction with the counterclockwise primary vortex. Furthermore, it should be noted that the number of biocubes hung over the right screen decreases dramatically compared to the neutrally buoyant case (See Fig. 4-(c)). Fig. 11 shows biocube distributions with time for the biocube density of 0.99g/cm^3. The process in which biocubes are attracted into the primary vortex is shown well in Fig. 11.

3.4 Effect of grid-resolution on the distribution pattern

As the last part of the present numerical study on fluid-particle mixture, the effect of grid-resolution on biocube distribution pattern is investigated using two different unstructured grid systems. Grid I consists of about 16,000 nodes and approximately 30 nodes are placed around the surface of each particle. Grid I has been used for all the results shown in Figs. 4~11. In order to conduct grid-resolution test, a coarse unstructured grid system (Grid II) has been used. Grid II consists of about 8,000 nodes and approximately 20 nodes are placed on the surface of each circle. Fig. 12 compares the particle distribution with time for two different grid systems. It is shown that the time evolution of biocube distribution for Grid II is very similar to that for Grid I. There-

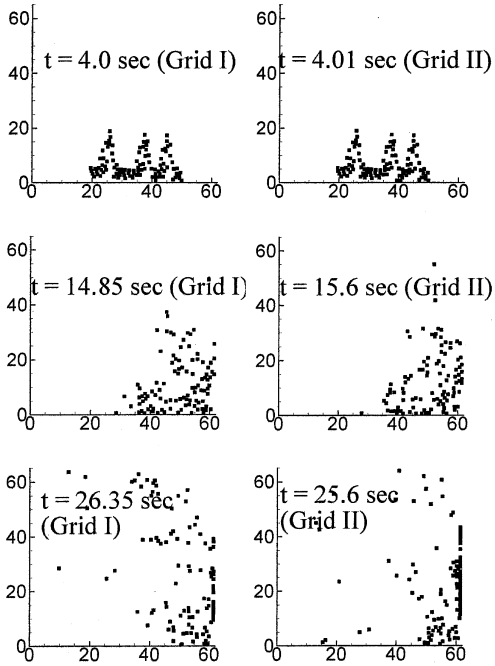

Fig. 12 Effect of grid-resolution on biocube distribution (Number of node of Grid I~16,000, Grid II~8,000)

fore, it can be said that present numerical results obtained using Grid I is quite close to a grid-independent solution.

4. Conclusion

From the two-dimensional direct numerical simulation of biocube-fluid mixture flow, which is used in sewage system, the following conclusions are obtained.

(1) It has been shown that air-bubbles ejected asymmetrically from the bottom induce a primary counterclockwise vortex, which is the essential ingredient for the uniform distribution of biocubes inside sewage reservoir.

(2) When a biocube density is slightly smaller than that of surrounding fluid or neutrally buoyant, most of biocubes in reservoir tend to reside in the primary counterclockwise vortex increasing the destruction rate of noxious chemicals than the case without air-bubble.

(3) Walls installed at the upper and lower part of the screen induce local vortices near the upper and lower part of the screen wall leading to the washout of biocubes residing near the screen wall.

(4) In the viewpoint of numerical modeling,

(a) The air-bubble ejected from the bottom of the reservoir is well modeled by momentum forcing imposed inside reservoir in the positive y-direction and its magnitude is selected depending on the rising velocity of air-bubble.

(b) Based on the assumption that surface tension and the normal velocity at free surface are negligible in the present problem, zero traction is used for x-momentum equation and $v=0$ is used for y-momentum equation.

(5) A parametric study on the optimal array of bubble-generating pipes as well as the intensity of air-bubble jet is to be conducted as a future study.

Acknowledgement

This work was supported by the research fund of Seoul National University of Technology. The authors are thankful to the reviewers for their helpful comments.

References

Ahn, S. W., Lee, B. C., Kim, W. C., Bae, M. W. and Lee, Y. P., 2002, "Characteristics of Fluid Flow and Heat Transfer in a Fluidized Heat Exchanger with Circulating Solid Particles," *KSME International Journal*, Vol. 16, No. 9, pp. 1175~1182.

Choi, H. G., 2000, "Splitting Method for the Combined Formulation of Fluid-Particle Problem," *Comput. Methods. Appl. Engrg.*, Vol. 190, pp. 1367~1378.

Choi, H. G. and Joseph, D. D., 2001, "Fluidization by Lift of 300 Circular Particles in Plane Poiseuille Flow by Direct Numerical Simulation," *J. Fluid Mech.*, Vol. 438, pp. 101~128.

Glowinski, R., Pan, T. W., Hesla, T. I. and Joseph, D. D., 1999, "A Distributed Lagrange

Multiplier/Fictitious Domain Method for Particulate flows," *Int. J. Multiphase Flow*, Vol. 25, pp. 755～794.

Hesla, T., 1990, "Combined Formulation for Fluid-Particle Mixture," unpublished note.

Hu, H.rH., 1996, "Direct Simulation of Flows of Solid-Liquid Mixture," *Int. J. Multiphase Flow*, Vol. 22, pp. 335～352.

Kim, D. W., 2002, "Improved Convective Heat Transfer Correlations for Two-Phase Two-Component Pipe Flow," *KSME International Journal*, Vol. 16, No. 3, pp. 403～422.

Kolon Engrg. & Construction Co., 2001, "Environmental New Technology No. 18 : Sewage treatment system using biocube," *Issued by Environmental Management Corporation*, WWW html document, address http://www.emc.or.kr/english/koetv/verification(box).htm

Lim, T. W. and Han, K. I., 2003, "A Study on Pressure Drop Characteristics of Refrigerants in Horizontal Flow Boiling," *KSME International Journal*, Vol. 17, No. 5, pp. 758～765.

Nam, Y. S., Choi, H. G., and Yoo, J. Y., 2002, "AILU Preconditioning for P2P1 Finite Element Formulation of the Incompressible Navier-Stokes Equations," *Comput. Methods. Appl. Engrg*., Vol. 191, pp. 4323～4339.

Sussman, M., Smereka, P., and Osher, S., 1994, "A Level set Approach for Computing Solutions to Incompressible Two-Phase Flow," *J. Comput. Phys*., Vol. 114, pp. 146～159.

Van der Vorst, H. A., 1992, "Bi-CGSTAB : a Fast and Smoothly Converging Variant of Bi-CG for the Solution of Non-Symmetric Linear Systems," *SIAM J. Sci. Statist. Comput*., Vol. 12, pp. 631～644.